www.czasopisma.pan.pl PAN POLSKA AKADEMIA NAUK www.journals.pan.pl

PAN ARCHIVES OF ACOUSTICS
Vol. **45**, No. 2, pp. 329–339 (2020)
DOI: 10.24425/aoa.2020.133153

Research Paper

Analysis for Improvement of Doppler Tomography Imaging of Objects Scattering Continuous Ultrasonic Waves

Tomasz ŚWIETLIK*, Krzysztof J. OPIELIŃSKI

Department of Acoustics and Multimedia, Faculty of Electronics
Wroclaw University of Science and Technology
Wybrzeże Wyspiańskiego 27, 50-370 Wrocław, Poland; e-mail: krzysztof.opielinski@pwr.edu.pl
*Corresponding Author e-mail: tomasz.swietlik@pwr.edu.pl

(*received November 8, 2019; accepted December 19, 2019*)

The paper describes an innovative ultrasound imaging method called Doppler Tomography (DT), otherwise known as Continuous Wave Ultrasonic Tomography (CWUT). Thanks to this method, it is possible to image the tissue cross-section *in vivo* using a simple two-transducer ultrasonic probe and using the Doppler effect. It should be noted that DT significantly differs from the conventional ultrasound Doppler method of measuring blood flow velocity. The main difference is that when measuring blood flow, we receive information with an image of the velocity distribution in a given blood vessel (Nowicki, 1995), while DT allows us to obtain a cross-sectional image of stationary tissue structure. In the conventional method, the probe remains stationary, while in the DT method, the probe moves and the examined tissue remains stationary.

This paper presents a method of image reconstruction using the DT method. First, the basic principle of correlation of generated Doppler frequencies with the location of inclusions from which they originate is explained. Then the exact process and algorithm in this method are presented. Finally, the impact of several key parameters on imaging quality is examined. As a result, the conclusions of the research allow to improve the image reconstruction process using the DT method.

Keywords: continuous wave ultrasonic tomography; Doppler tomography; image reconstruction.

1. Introduction

The Doppler tomography method allows to image the cross-section of the object interior (or a tissue structure) by using a moving two-transducer probe generating and receiving a continuous ultrasonic wave. Let us assume that the probe generates a wave with the frequency f_T. Bearing in mind the Doppler effect, we can also assume that the wave reflected from a given inclusion in the quasi homogeneous object cross-section is equal to f_R. Seeing that the Doppler frequency f_d generated by the inclusion adds (or subtracts from) the transmitted frequency, it can be stated that $f_d = f_T - f_R$. It is obvious that the frequency cannot be negative, but for our applications, we assume that the Doppler frequency is positive when the inclusion at the time of measurement moves towards the probe. Otherwise the frequency f_d is negative.

Two types of geometry can be distinguished in which the ultrasonic probe can move (Liang *et al.*, 2001; 2011). It is worth noting that in both cases, the examined tissue as well as the moving probe are immersed in distilled water. The first type is the linear geometry. In this case, the ultrasonic probe archives data moving along the tested object (Fig. 1a). The second type is the circular geometry, where the probe moves around the imaged object cross-section (Fig. 1b). For this particular case, DT can be used, among others, to examine and reconstruct the image of cancer inclusions inside the female breast. The method can also be used to image limb bones, for example in the event of fractures.

This paper focuses on the DT method in the circular geometry. In this case, the Doppler frequency for a single inclusion located at a distance r and the position of the probe at an angle θ can be calculated by the formula (1):

$$f_d = 2 \cdot f_T \cdot \omega_{\text{turn}} \cdot r \cdot \frac{\cos(\theta)}{c}, \tag{1}$$

where ω_{turn} is the frequency of the probe rotation around the imaged object, c is the ultrasonic wave speed in the examined object (tissue).

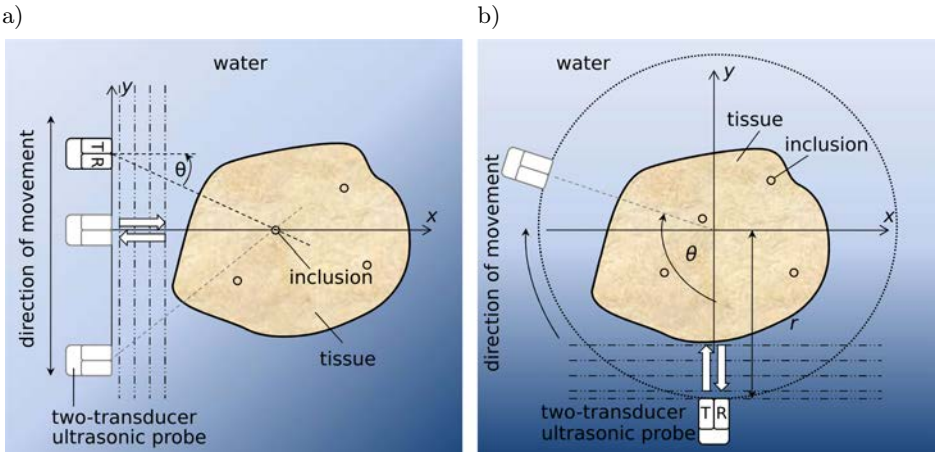

Fig. 1. DT measuring system for: a) linear geometry and b) circular geometry.

2. Acquisition of signals

In order to simplify and facilitate understanding of the idea of image reconstruction for the DT method in circular geometry, we assume that the probe is stationary and the tested object is rotated. From the point of view of using this method, it is obviously impractical, but it allows easier visualisation of the basic principles of this method. As for the generated Doppler frequencies, they are the same when the source is moving (probe) and the tested object is stationary, as well as in the opposite case.

We assume that inside the imaged object there are three inclusions marked a, b, c, as shown in Fig. 2a. In the first step we should determine the velocity components for each inclusion in the direction of propagation of the ultrasonic wave for a given angle of rotation. In this case, for a rotation angle of 0°, the values of the linear velocity components are: V_a, V_b, and V_c (Fig. 2a). By transforming formula (1), it can be seen that each of these velocities are correlated with a Doppler frequency. In this case, the Doppler frequencies are: f_{da}, f_{db}, f_{dc}, respectively. Depending on the direction in which the ultrasonic probe moves, the frequency has a sign (+) or (−). We assume that when the scatterer moves towards the probe we have the sign (+), otherwise it is the sign (−).

There are two facts that are crucial when it comes to understanding the basic idea of image reconstruction for the DT method. First of all, it should be noted that the velocity components V increase their value as they move away from the centre of rotation (Fig. 2b). Secondly, on the lines in the direction of ultrasonic wave propagation velocity values are the same (see Fig. 2b on the example of V_c velocity). By transforming formula (1) it can be concluded that the same

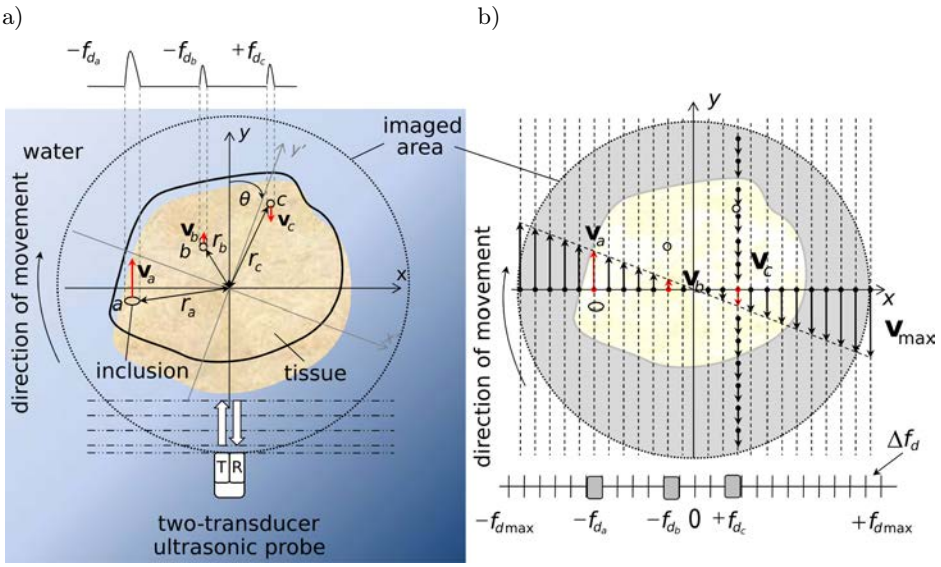

Fig. 2. Example of three inclusions within the imaged object structure together with V velocities and f_d frequencies (a) and the illustration of the basic relationships of velocity V and f_d inside the imaged zone (b).

principles apply to Doppler frequencies correlated with the velocity components V. Additionally, based on the maximum velocity in the imaging area $V_{\max}$, the maximum Doppler frequency $f_{d\max}$can be calculated.

The next step in the image reconstruction using the DT method is to create a Doppler frequency range $(-f_{d\max};\ +f_{d\max})$. This range is divided into bands hereinafter referred to as Doppler bands of equal width Δf_d (Fig. 2b). For a given angle θ we can define the sum of Doppler frequency amplitudes into each band. When we perform this operation for each angle of rotation θ we get a matrix which in rows contains the sums of frequency amplitudes for individual Doppler bands, while in the columns the angle of rotation changes. This matrix is called a sinogram (Kak, Slaney, 1988). In the geometry of parallel-radial projections, it can be directly used to reconstruct the cross-sectional image of the examined object by the methods used in X-ray tomography (Opieliński, Gudra, 2010).

The last stage of image reconstruction process is the application of one of the algorithms used in computed tomography. In this paper, a fast algorithm called filtered back projection (FBP) was used. It is worth noting that this algorithm allows reconstruction of the full image based on half of the data from the turnover.

In order to present the image reconstruction from simulated data, we consider the case of a rotating platform on which a single scatterer was placed (Fig. 3a). It is infinitely small and scatters the ultrasonic wave in every direction in the same way. This inclusion is set at a distance of 3 cm from the centre of rotation and at an angle of 0° to the probe. Other simulation parameters are: ω_{turn} = 2 turns per second; speed of ultrasound around the scatterer c = 1482 m/s; f_T = 4.7 MHz; number of angles θ per half turn equals to 200; the number of Doppler bands is 125, within a 10 cm diameter imaging area. Figure 3b shows a sonogram in which the Doppler bands which contain the Doppler frequency at a given angle of rotation of the scatterer are marked in white. Figure 3c shows an image reconstructed on the basis of the mentioned sinogram.

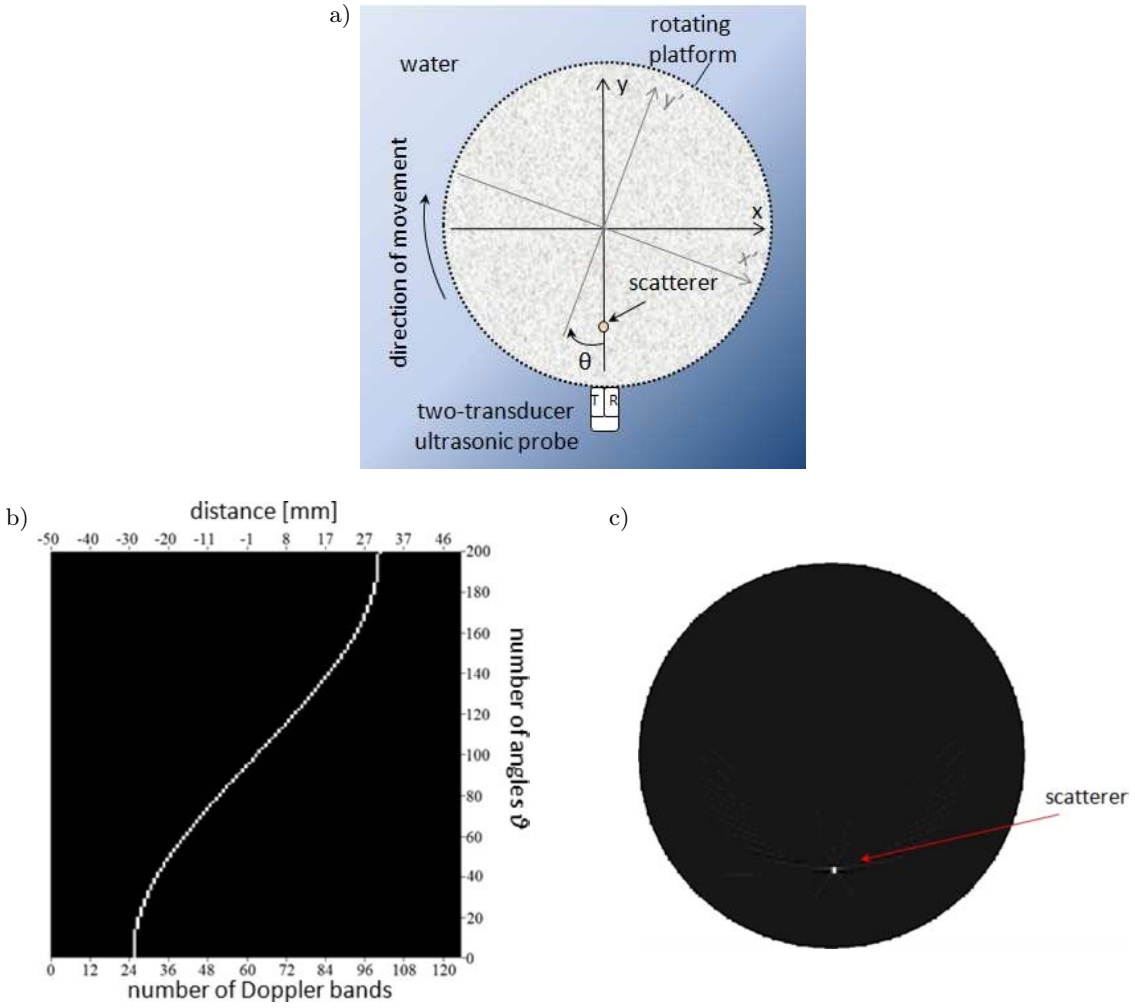

Fig. 3. Simulation of a scatterer placed on a rotating platform (a), example of the sinogram created for the moving scatterer (b), reconstruction of the scatterer image (c).

3. Filtered back projection algorithm

The FBP algorithm is based on the assumption that the measurement for a single so called projection can be treated as a two-dimensional filtering operation in the spatial frequency domain (Kak, Slaney, 1988). For the general case, the measurement data are continuous functions, and their argument is the normalised distance of the probe from the centre of the axis of rotation of the imaged object. However, for the purposes of the DT method, they must be converted to a discrete form. This necessitates the use of a discrete Fourier transform (Kak, Slaney, 1988).

For our needs, it is required to determine the maximum frequency of Doppler frequency amplitude changes. Let us denote this value by W. In addition, two quantities should be specified for the FBP algorithm. The first one is the so called number of projections marked as N_p. For the DT method, it is the number of rotation angles θ of the ultrasonic probe (or test object). The second parameter is the number of M_p rays and they correspond to the number of Doppler bands. Based on Nyquist's theorem, it can be seen that the values of projection $p_\theta\ (mT)$ should be sampled with the period $T = 1/(2W)$, where $m = -N/2, ..., 0, (N/2) - 1$, for cases of sufficiently large N. When the algorithm is used in the DT method, the period T corresponds to the bandwidth Δf_d.

To reconstruct the image, in the first step, based on the formula (2), the approximation of the Fourier transform $S_\theta(w)$ should be determined for each projection. For the DT method, it is a discrete function of the frequency of changes in Doppler frequency amplitude for individual rotation angles θ (Świetlik, Opieliński, 2019):

$$S_\theta(w) \approx S_\theta\left(m\frac{2W}{N}\right) = \frac{1}{2W}\sum_{k=-\frac{N}{2}}^{\frac{N}{2}-1} p_\theta\left(\frac{k}{2W}\right)\cdot e^{j2\pi\left(\frac{mk}{N}\right)}, \quad (2)$$

where N is the number of projection samples equal to the number of measurement rays M_n. Due to the use of FFT, the N parameter should be the power of 2. If this is not the case, N increases to the value of the nearest power of 2, remembering that additional samples have the value of 0.

In the next step, all projections are filtered in the frequency domain and multiplied by a window function (e.g., Hamming window). This allows us to eliminate noise in the reconstructed image (Kak, Slaney, 1988). The formula (3) should be used for this purpose (Świetlik, Opieliński, 2019):

$$Q_\theta\left(\frac{k}{2W}\right) \approx \left(\frac{2W}{N}\right) = \sum_{m=-\frac{N}{2}}^{\frac{N}{2}} S_\theta\left(m\frac{2W}{N}\right)\cdot\left|m\frac{2W}{N}\right| \cdot H\left(m\frac{2W}{N}\right)\cdot e^{j2\pi\left(\frac{mk}{N}\right)}, \quad (3)$$

where $k - N/2, ..., 0, ..., N/2$, and $H(m(2W/N))$ is a window function.

The last stage is the reconstruction of the image by means of the back projection using the formula (Świetlik, Opieliński, 2019):

$$f(x,y) = \frac{\pi}{K}\sum_{i=1}^{K} Q_{\theta_i}(x\cdot\cos\theta_i + y\cdot\sin\theta_i), \quad (4)$$

where $K = N_p/2$, which means that half of the full rotation angles θ are sufficient for reconstruction. A more detailed description of this algorithm is presented in the paper by Świetlik and Opieliński (2019).

4. Doppler signal simulation

The Doppler signal is the most important signal in the DT method and consists only of Doppler frequencies. It can be determined on the basis of the product of the transmitted and received signal at a given rotation angle θ and the simultaneous use of a filter that will eliminate all frequencies above the maximum Doppler frequency. This signal is of the chirp type, therefore it can be written in the form of $s(t) = A\cdot\sin(\varphi(t))$, where A is the signal amplitude, and $\varphi(t)$ is an unknown modulating function (Świetlik, Opieliński, 2019). The frequency of this signal is equal to (Świetlik, Opieliński, 2019):

$$f(t) = \frac{1}{2\pi}\frac{d\varphi(t)}{dt}. \quad (5)$$

Based on the formula (1), it can be seen that the Doppler frequency for a single insertion changes according to the formula (Świetlik, Opieliński, 2019):

$$f(t) = \frac{4\pi\cdot f_T\cdot f_{\text{turn}}\cdot r_0\cdot\cos\left(2\pi\cdot f_{\text{turn}}\cdot t + \alpha_0\right)}{c}, \quad (6)$$

where r_0 is the distance between the inclusion and the centre of rotation, α_0 is the angle at which the inclusion is set in relation to the ultrasonic probe at a 0° angle of rotation, f_{turn} is the frequency of rotation of the probe (or tested object). By comparing formulas (5) and (6), we can determine the value of $\varphi(t)$, and thus the formula for a Doppler signal is (Świetlik, Opieliński, 2019):

$$s(t) = A\cdot\sin\left(\frac{4\pi\cdot f_T\cdot r_0}{c}\cdot a^*\right), \quad (7)$$

where

$$a^* = \left(\sin\left(2\pi\cdot f_{\text{turn}}\cdot t + \alpha_0\right) - \sin\alpha_0\right).$$

In order to calculate the signal from several inclusions, we must first calculate the values for individual scatterers, and then sum up the values for the respective t times.

5. Basic problems of DT image reconstruction

One of the basic problems with measuring data acquisition in the DT method is the need to register data for each angle θ separately. This necessitates a very good synchronisation of the ultrasonic probe rotation with measurements and switching on of the probe even several hundred times per minute. A simple solution to this problem is the acquisition of a Doppler signal from the full rotation of the probe (or tested object) and the division of this signal into individual rotation angles θ programmatically.

The second, much more difficult, problem to solve is the need to ensure adequate Doppler spectrum resolution for individual rotation angles θ. Consider again the example from Sec. 2 of a single scatterer placed on a rotating platform at a distance of 3 cm from the centre of rotation axis and at an angle of 0° to the probe (Fig. 3a). The simulation assumes that we have 200 angles for half a turn or 398 angles for the whole turn. Such a quantity ensures the correct accuracy of image reconstruction. In addition, it was assumed that we have 10 000 samples, formula (7) was used and the Doppler signal was calculated. In the next step, it was calculated that if we divided this signal into equal 398 sections for respective angles θ, each of them would contain 51 samples. The number of samples should be 50, but increased by 1 so as to obtain the odd number and as a result to determine the centre of the given angle θ in an easier manner. This procedure facilitates image reconstruction. The sampling period of the Doppler signal is 25 μs, which gives a sampling frequency of f_s = 40 kHz. As a result, the spectrum resolution for a single angle θ is equal to Δf = 784 Hz. Due to the diameter of the imaging zone, the maximum Doppler frequency in this case is equal to $f_{d\max}$ = 3984 Hz based on the formula (2). From this it follows that only 11 Doppler bands can be determined in this case. Such a small value means that we do not have enough information in the sinogram to reconstruct the image with a good resolution. In this case, the image has a resolution of 11×11 pixels, which gives the large surface about 1 cm^2 for one pixel.

In this situation, it seems reasonable to increase the number of samples. For example, let us increase the number of samples twice, to 20 000. This causes the signal sampling period to decrease to 12.5 μs (f_s = 80 kHz), and the number of samples to increase to 101. However, the spectrum resolution remains at a similar level and is equal to Δf = 792 Hz. This again allows us to determine only 11 Doppler bands and causes no improvement in image resolution.

The effect of the lack of resolution improvement results from the formula (8). If in the Doppler signal for a given rotation angle θ we increase the number of samples N, we simultaneously increase the sampling frequency f_s. As a result, the ratio of these quantities remains the same:

$$\Delta f = \frac{f_s}{N}. \tag{8}$$

6. Overlay algorithm

The solution to the problem with the resolution of the Doppler spectrum for individual rotation angles θ described in Sec. 5 may be the overlay algorithm. Its idea is to increase the length (number of samples N) of the Doppler signal for rotation angles while leaving the sampling rate f_s at the same level. In this situation, Δf decreases and the spectrum resolution improves. With equal division of samples into individual rotation angles, the increase in N requires adding data from adjacent Doppler signal ranges. This results in intervals for the rotation angles in the parts overlap. Figure 4 presents the process, on the example of angles θ_i and θ_{i+1}. Parameter α corresponds to the length of the Doppler signal for rotation angles θ and is the same for each of them. It is given in relation to the full rotation of the probe or the tested object in degrees.

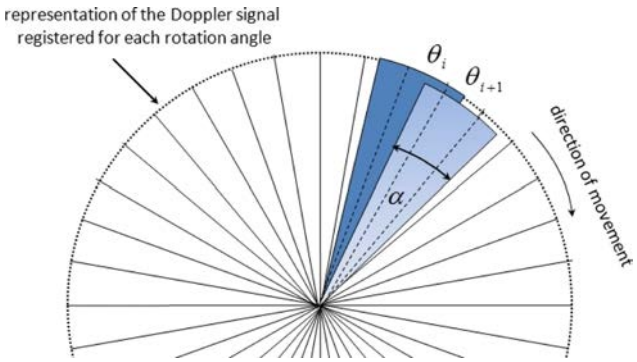

Fig. 4. Idea of Doppler signal overlay algorithm for rotation angles θ_i and θ_{i+1}.

Depending on the α parameter, we obtain a different spectrum resolution Δf, which directly affects the accuracy of Doppler frequency determination, which in turn affects the quality of the reconstructed image. Figure 5 presents the results of a simulation showing the spectrum for a single inclusion placed on a rotating platform at a distance of 3 cm from the centre of rotation and at an angle of 0° in relation to the probe for various parameters α. The conditions of the experiment are the same as those described in Sec. 2, with the difference that 25 000 samples were generated for the Doppler signal calculated from formula (7). In addition, it should be noted that the spectra are calculated for a Doppler signal slice for the rotation angle θ = 0°. In this simulation, α took the values: 1.8°, 3.6°, 5.4°, 7.2°, 9.0°, 10.8°, 12.6°, 14.4°, 16.2°, 18.0°. The spectral resolution values for each case were also calculated. The Δf values are: 398.39 Hz, 199.59 Hz, 133.15 Hz, 99.90 Hz, 79.93 Hz,

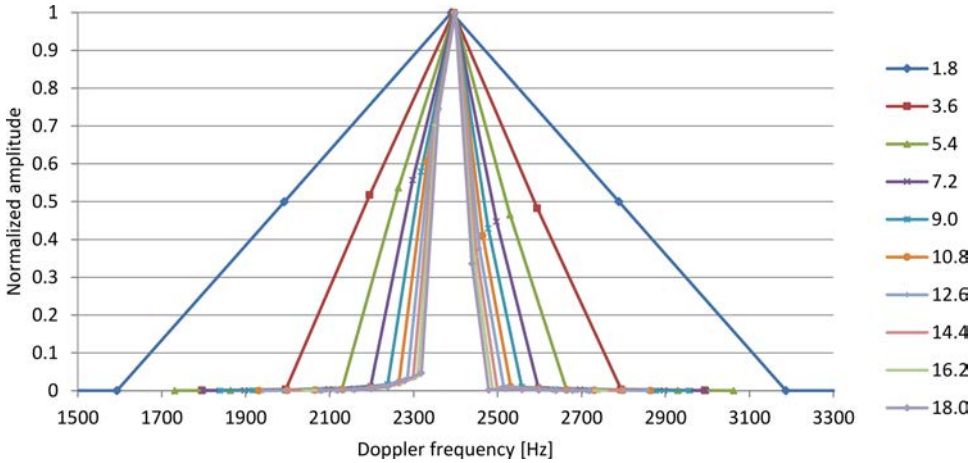

Fig. 5. Dependence of the Doppler signal resolution for the rotation angle $\theta = 0^\circ$ of a single inclusion from the parameter α.

66.62 Hz, 57.14 Hz, 49.97 Hz, 44.42 Hz, 39.98 Hz, respectively. On the basis of the presented values and on the basis of Fig. 5 it is very clear that the higher the value of the α parameter, the better the spectrum resolution. It can also be seen that the greatest improvement is obtained for α in the range $(1.8^\circ; 9.0^\circ)$. For larger α the value of Δf decreases relatively slower.

7. Influence of particular parameters of the DT method and overlay algorithm on image reconstruction quality

The two most important parameters having the greatest impact on the quality of imaging in the DT method are the number of acquisition angles and the number of Doppler bands. It should be noted that using the overlay algorithm, the number of Doppler bands is closely related to the value of the parameter α.

The number of Doppler signal acquisition angles N_θ affects the coordinates of the imaged inclusions. In order to demonstrate this effect, a simulation was performed of scanning DT signals from a single point located on the rotating platform at a distance of 3 cm from the centre of rotation and set at an angle of 0° in relation to the probe. The overlay algorithm was used where the parameter $\alpha = 9^\circ$. The Doppler signal recorded at half rotation has 25 000 samples. Other simulation parameters are the same as those given in Sec. 2. Figure 6 shows DT image reconstruction results for changing the number of acquisition angles N_θ from 20 to 200. The dimension of each image section is 11.22×15.30 mm. A pixel with a red frame represents the place where in the perfect case the centre of the inclusion image should be reconstructed. The first conclusion is that for a small number $N_\theta \in (20; 100)$ a fairly large error in the reconstruction of the inclusion coordinates appears. In addition, for $N_\theta = 20$ and 40, significant interference in the reconstruction of the image in the form of additional dark pixels around the inclusion image should be noted.

In order to further investigate the error, the distance from the centre of the reconstructed point to the place where it should be located in the ideal simulation was calculated. In addition, the range of tested N_θ

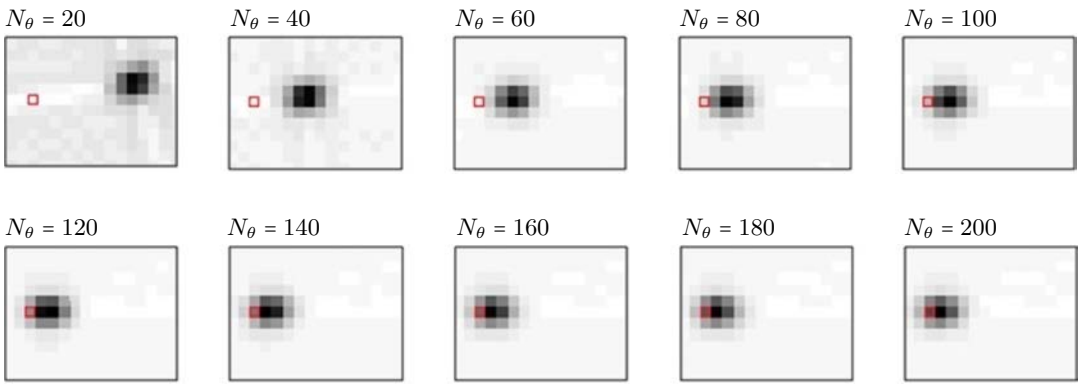

Fig. 6. Dependence of the point image reconstruction on the number of acquisition angles N_θ.

values was increased to 500, and the results are shown in Fig. 7. The data from the graph confirms that the largest errors in the inclusion position reconstruction are for $N_\theta \in (20; 100)$. For a value between 140 and 400, the error has a value of about 1 mm, while at a value of 500 it drops to zero.

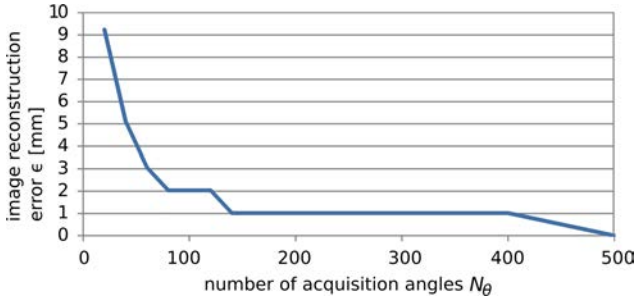

Fig. 7. Dependence of the reconstruction error of inclusion coordinates on the number of acquisition angles N_θ.

One of the more important conclusions from the previous experiment is the fact that for a number of acquisition angles of 500 and above, we do not obtain an error in reconstructing the position of the inclusion image. The next simulation should examine whether and how the parameter α from the overlay algorithm affects the reconstruction of the image of points located in different places of the imaging area. To this end, images of inclusions located at a distance of 5 mm from the centre of rotation and set at selected angles relative to the probe were reconstructed. For this simulation, the α parameter was increased to 14.4°. The results are shown in Fig. 8. It is worth noting that as the inclusion moves away from the centre of rotation, the length of its image across increases. This is the result of using the overlay algorithm. The influence of the α parameter on the inclusion image resolution is discussed in detail later. However, at the moment it can be stated that

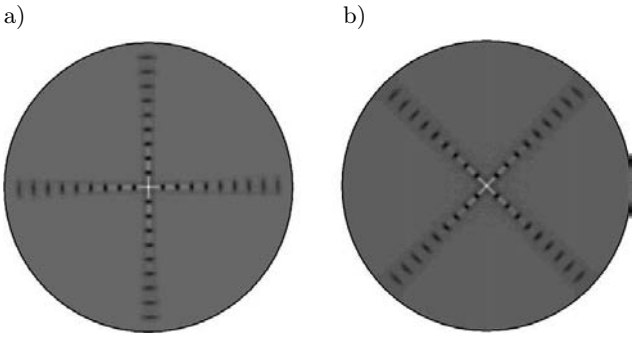

Fig. 8. Image reconstruction of inclusions placed at a distance of 5 mm from the centre of rotation and at an angle in relation to the probe: a) 0°, 90°, 180°, 270°, b) 45°, 135°, 225°, 315°.

for optimal determination of the α parameter for the entire imaging area, the image resolution for the point furthest from the centre should be examined, because it will be the worst there.

Images at 0° and 180° were examined to accurately analyse inclusion images. The idea of the measurements is presented in Fig. 9. The resolution was tested along and across the image of an example inclusion sample located 35 mm from the centre of rotation and located at an angle of 180° to the probe (Fig. 9a). Other simulation parameters remain unchanged. Analysing pixel values for individual images, it was assumed that the resolution will be tested with a 3 dB decrease in the maximum pixel value (Figs 9b and 9c). In addition, inclusion blur was tested assuming that it would the 10% of the maximum pixel value (Figs 9b and 9c). The test results for all 18 inclusion images are shown in Fig. 10. Both on the basis of these results and on the basis of Fig. 8, it can be seen that the inclusions located at the same distance from the centre of the image are symmetrical and have the same longitudinal and transverse resolutions. It should also be

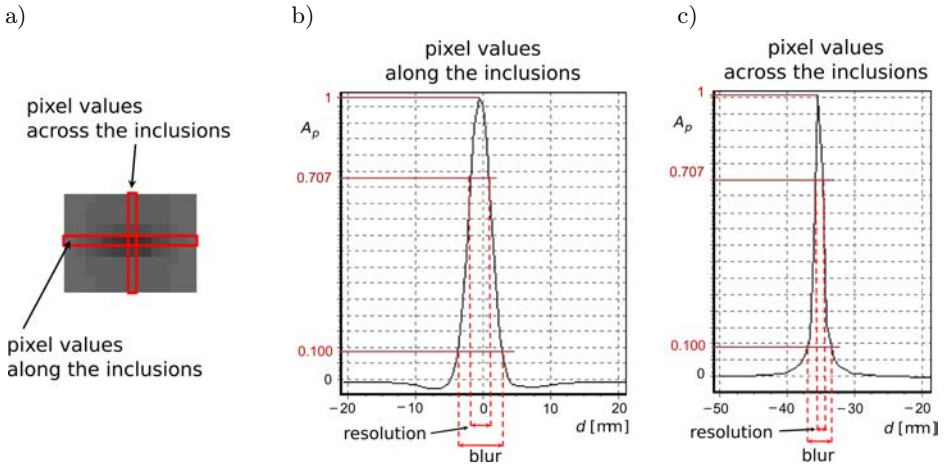

Fig. 9. Idea of measuring pixel values along and across the inclusion image located 35 mm from the centre of rotation and at an angle of 180° to the probe (a). Example of measuring resolution and blur along image inclusion (b). Example of measuring resolution and blur across image inclusions (c).

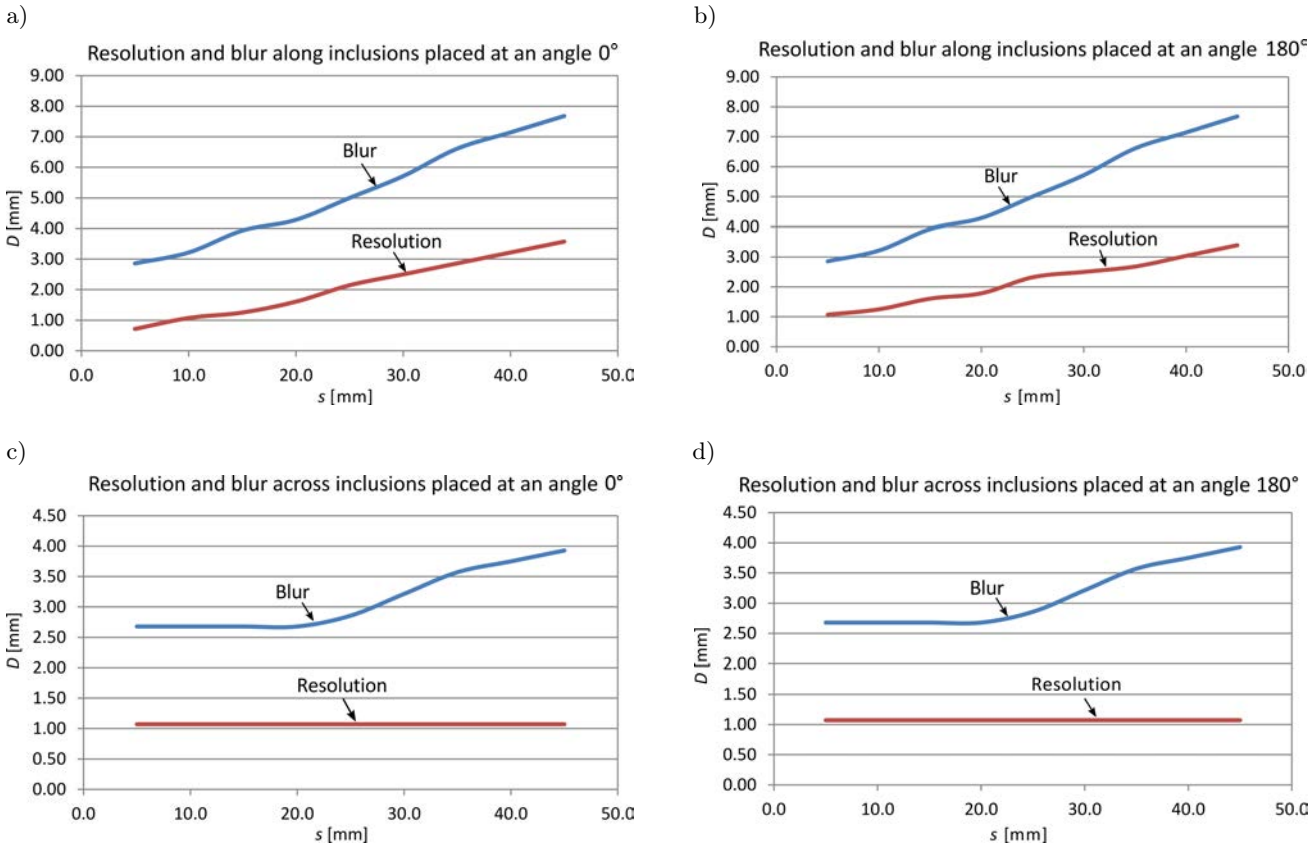

Fig. 10. Resolution and blur along and across inclusions placed at an angle of 0° and 180°.

noted that the resolution and blur along the inclusions increase in line with the distance from the centre of the image (Figs 10a and 10b). Bearing in mind that we simulate the image of infinitely small inclusions, it can be seen that closer to the centre we can reconstruct images with fairly good resolution of about 1 mm and blur at the level of 3 mm.

In extreme cases, near the edge of the image, resolution up to about 3.5 mm, and blur up to about 7.5 mm is noticed and this is still a good result. As far as the resolution across the inclusions' image is concerned, it remains the same regardless of the distance between the scatterer and the centre of the image and for this test it is equal to about 1 mm (Figs 10c and 10d). In the case of blur, it is also constant for inclusions close to the centre, but then increases to the value of about 4 mm (Figs 10c and 10d).

In the next simulation the dependence of the inclusion image resolution on the α parameter from the overlay algorithm was measured. An inclusion 4.5 cm from the centre of rotation was chosen because of the highest resolution and blur values at the edge of the image. This would allow the worst case imaging to be examined and would give the opportunity to determine the optimal α parameter for the entire imaging area. A larger distance from the centre point would result in the image being cut off in some simulation cases. It should also be noted that the angle at which the measured inclusion is set does not matter because we have the same longitudinal and transverse resolutions for inclusions at the same distance from the centre of the image. Therefore, in order to simplify measurements, the angle of 0° was chosen. The α parameter took the following values: 1.8°, 3.6°, 5.4°, 7.2°, 9°, 10.8°, 12.6°, 14.4°, 16.2°, 18°. Other simulation parameters remained the same.

In order to examine the impact of overlay algorithms in the DT method, we first simulated the so called perfect case (with the simulation of Doppler frequencies directly) for whose imaging this algorithm was not used. In this case, we used the formula (1) to calculate Doppler frequencies. As a result, we eliminated errors in determining this frequency. The simulation results are shown in Fig. 11. Each image section is 15×15 mm. Image reconstruction was possible because for each value of the α parameter from the so called real simulation, the number of Doppler bands was calculated. They are equal to, respectively: 21, 39, 59, 79, 99, 119, 139, 159, 179, 199. It can be clearly seen in Fig. 11 that the higher the number of Doppler bands, the better the image resolution (Świetlik, Opieliński, 2016). This effect was thoroughly examined by the method presented in Fig. 9, and the results are shown in Fig. 13.

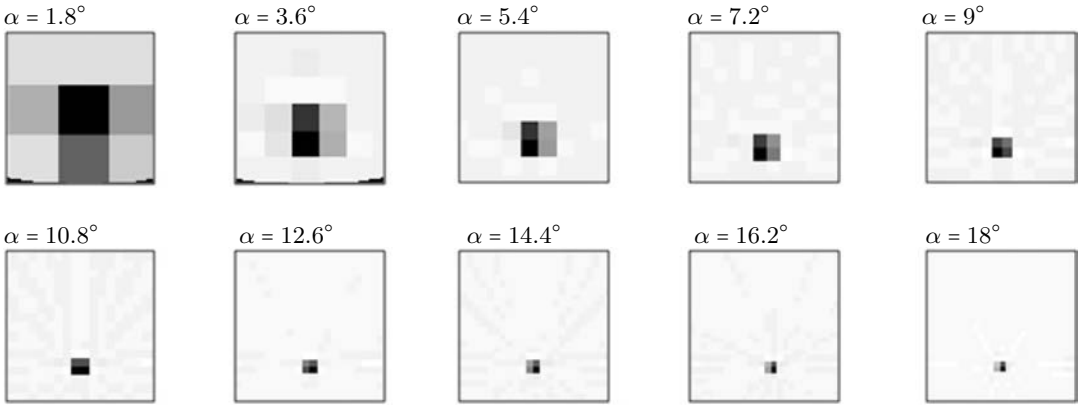

Fig. 11. Simulation of the perfect case of inclusion image reconstruction for selected values of the number of Doppler bands corresponding to the α parameters.

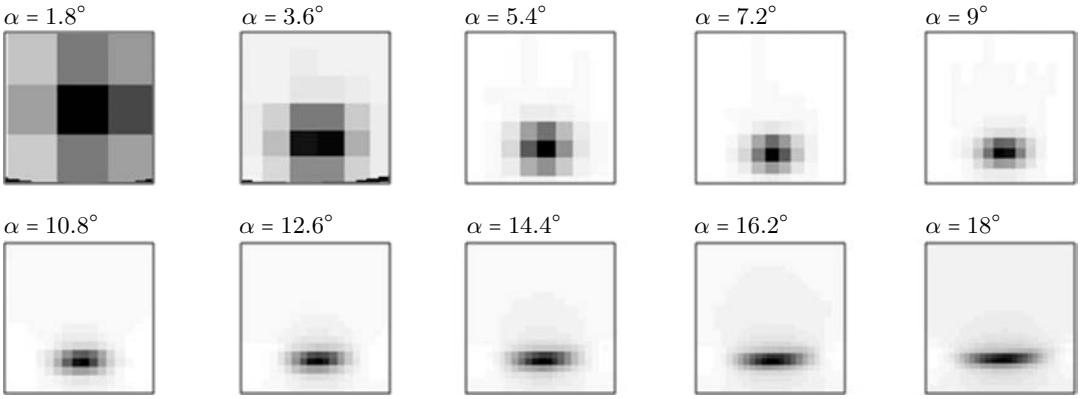

Fig. 12. Simulation of the real case of inclusion image reconstruction for selected values of α parameter.

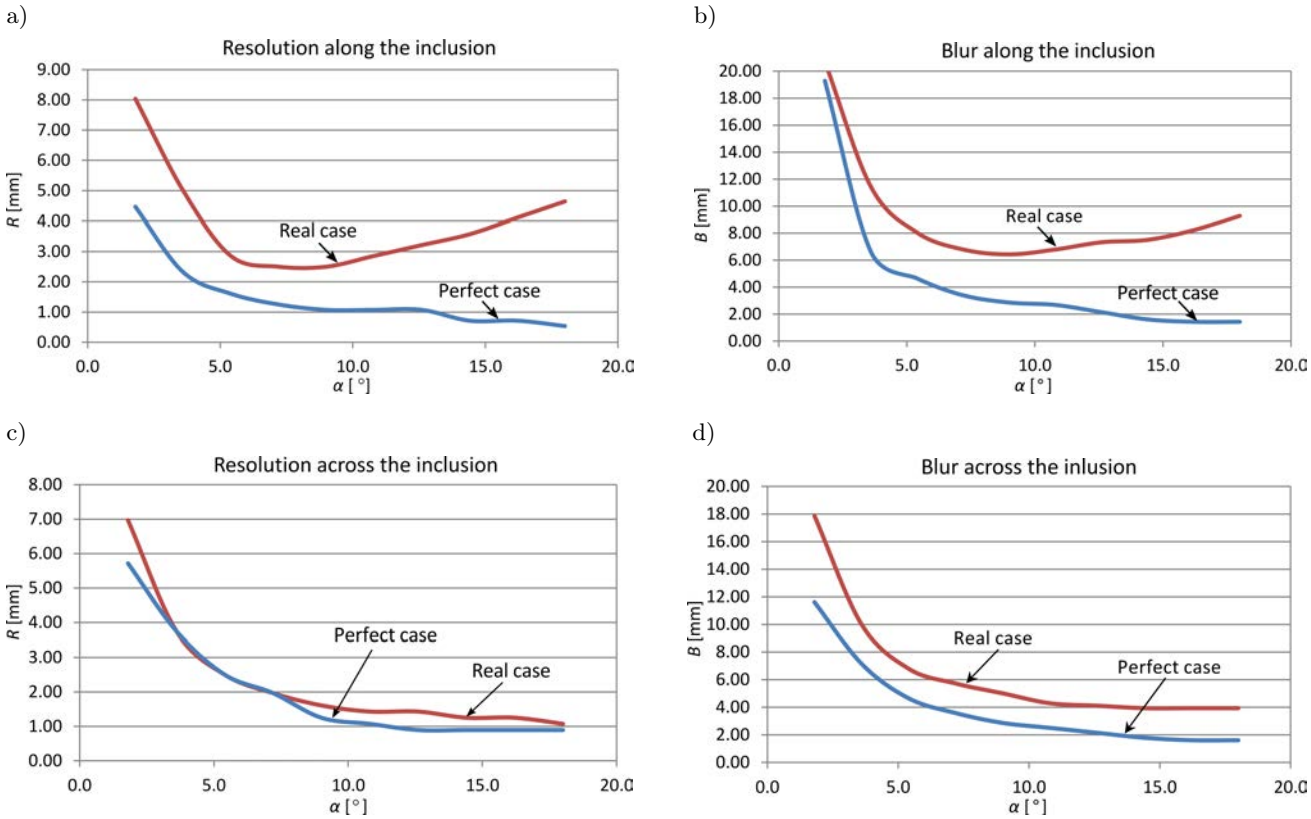

Fig. 13. Resolution and blur along and across inclusions for the perfect and real cases of simulation.

In the second real case with the simulation of full scattered signals, the inclusion images were reconstructed using an overlay algorithm. The results are shown in Fig. 12. As before, each image section has a dimension of 15×15 mm. In this case, you can also see an improvement in resolution as the α parameter increases. However, in contrast to the perfect case for values above $\alpha = 9°$, the image elongation along the inclusion is clearly visible. The resolution and blur of the image were measured accurately along and across the inclusion by the method presented in Fig. 9, and the results are shown in Fig. 13.

Analysing Fig. 13, it can be seen that both resolution and blur across the image of the inclusion for the perfect and real case do not differ significantly. As the α parameter increases, the resolution decreases from around 7 mm to 1 mm in both cases. When it comes to blur, the values for the real case are on average 2 mm larger than those for the perfect case. The blur value drops from about a dozen mm for small α to a single mm for larger values of this parameter.

We have a completely different situation for the resolution and blur measured across the inclusion image. For the real case, it can be observed that after noting a decrease for small α at a value of about 9°, we observe an increase in both the value of resolution and blur. When it comes to the perfect case, notice a similar decrease in value as it was for the study of pixels across the image. The conclusion that comes to mind is that the value of parameter α should not exceed 9°, but at the same time it should be as high as possible to ensure good resolution and low image blur.

8. Conclusions

Doppler tomography is a relatively new method of imaging tissue cross-section *in vivo*, but in combination with the fast FBP image reconstruction algorithm it can give good results. However, we have to keep in mind the limitations of this method. First of all, attention should be paid to obtaining adequate resolution of the Doppler signal spectrum for a single viewing angle θ. With the classic division of the Doppler signal from the full rotation of the probe (or tested object) into the number of acquisition angles N_θ, we obtain insufficient resolution Δf. The solution to this problem may be the application of an overlay algorithm that allows a significant improvement in spectrum resolution, and thus more accurate determination of Doppler frequencies using the appropriate α parameter. It should be remembered that these frequencies are crucial when it comes to image reconstruction in the DT method.

The three parameters which have the greatest impact on image quality are the number of N_θ acquisition angles, the number of Doppler bands and parameter α from the overlay algorithm. As for the number of N_θ angles, it has the greatest impact on the accuracy of reconstructing the position of a given inclusion in the imaged section. If this parameter is too small and has values of e.g. 20, the image will be reconstructed even 9 mm further than it is in reality. With N_θ values above 120, the error decreases to 1 mm, while with a value above 500 it is equal to zero. So, to avoid an error in the insertion coordinate imaging, it should use 500 or more acquisition angles.

In the case of the number of Doppler bands and the α parameter, the image resolution changes. If the values of these parameters are too small, the resolution of the reconstructed inclusion is low, which can be seen in Figs 11 and 12. This relationship results, among others, from the fact that by dividing the frequency range from $-f_{d\max}$ to $+f_{d\max}$ into Doppler bands we are able to more accurately determine the value of the Doppler frequency when we have more bands. This also translates into more columns in the sinogram, which gives better resolution after using the FBP algorithm. However, research shows that the alpha parameter cannot be too large because there is image elongation along the inclusion. To prevent this, average values of this parameter should be used. In the cases described, it was $\alpha = 9°$. To determine the α parameter, it should be also remembered that the elongation of the inclusion image increases with the distance from the centre of the image. Therefore, to determine this parameter for the entire imaging area, inclusions close to the zone boundary should be tested.

Analysing the results of the described simulations, it can be stated that the DT method allows imaging of inclusions that have a relatively small diameter of about 2 mm to 3 mm. The blur of such an image is not more than 7 mm. Thus, this method could be used to screen for cancerous inclusions inside female breasts. Another possible way to use this method is bone imaging, e.g., in the case of fractures due to the high reflection coefficient of the ultrasonic wave.

References

1. Liang H.-D., Halliwell M., Wells P.N.T. (2001), Continuous wave ultrasonic tomography, *IEEE Transactions on Ultrasonics, Ferroelectrics, and Frequency Control*, **48**(1): 285–292, doi: 10.1109/58.896141.

2. Liang H.-D., Tsui Ch.S.L., Halliwell M., Wells P.N.T. (2011), Continuous wave ultrasonic Doppler tomography, *Interface Focus*, **1**(4): 665–672, doi: 10.1098/rsfs.2011.0018.

3. Kak A.C., Slaney M. (1988), *Principles of Computerized Tomographic Imaging*, IEEE Press, New York.

4. Świetlik T., Opieliński K.J. (2016), The use of Doppler effect for tomographic tissue imaging with omnidirectional acoustic data acquisition, [in:] Piętka E. *et al.* [Eds], *Information technologies in medicine. Advances in intelligent systems and computing*, Springer International Publishing, Switzerland, **471**: 219–230, doi: 10.1007/978-3-319-39796-2_18.

5. Świetlik T., Opieliński K.J. (2019), Analysis of the possibility of Doppler tomography imaging in circular geometry, [in:] Piętka E. *et al.* [Eds], *Information technologies in medicine. Advances in intelligent systems and computing*, Springer International Publishing, Switzerland, **762**: 52–63, doi: 10.1007/978-3-319-91211-0_5.

6. Nowicki A. (1995), *Fundamentals of Doppler ultrasonography* [in Polish: *Podstawy ultrasonografii dopplerowskiej*], Wydawnictwo Naukowe PWN, Warszawa.

7. Opieliński K.J., Gudra T. (2010), Ultrasonic transmission tomography, [in:] *Industrial and biological tomography – theoretical basis and application*, J. Sikora, S. Wójtowicz [Eds], Warsaw, Electrotechnical Institute.